International Journal of Scientific Research and Engineering Development-– Volume 7 Issue 3, May-June 2024
Available at www.ijsred.com

RESEARCH ARTICLE OPEN ACCESS

Hydrogeophysical Characterization and Prospect of Sandstone Aquifer in Delta South Parts of Delta State, Nigeria

[1]Ogwah C., Nnabo, P.N.,[1] Ezekiel O. I., [2]Atome, O. E
[1]Department of Geology, Faculty of Science, Ebonyi State University, Abakaliki, Ebonyi State Nigeria
[2]Department of Geology, Faculty of Science, Delta State University of Science and Technology, Ozoro Delta State, Nigeria

Abstract:
Groundwater management was the goal of the assessment of the geo-electric characteristics of the granular sandstone aquifer in Isoko and Patani and its surroundings. The Schlumberger electrode array was used for vertical electrical sounding (VES), with a maximum half-current electrode separation of 400 m. The region is distinguished by four to five geo-electric subsurface layers, according to the interpretation of the VES data. The evaluation of aquifer protective capacity was based on the following Dar-zarrouk parameters: longitudinal conductance (S), transverse resistance (T), longitudinal resistance (ρL), and transverse unit resistance (Tr).Results obtained from VES data suggested that the layer model ranges from 3 to 6 layers. It was observed that curve HA was the dominant curve type when compared to other curve types. Contour maps of iso-resistivity revealed that as AB/2 increases with depth from 6 to 150 m, the area becomes clayey.

Keywords: resistivity, sandstones, longitudinal conductance, aquifer protective capacity

Introduction:

Aquifers are geologic formations made up of the spaces between soils and weathered or fractured rocks that contain groundwater. Because groundwater's chemical and biological qualities are often consistent and require little treatment, it is frequently used for residential and commercial purposes because it is typically cleaner and free of contaminants than surface water (Akakuru et al., 2023; Eyankware et al., 2024). The significance of groundwater to human existence is immense; it is essential for home and industrial operations, sanitation, and crop production. However, over time, the aquifer has been overstretched due to mining activities, sewage from latrines, underlined petroleum pipes, septic tanks, leaks from surface and underground storage, oil spills, movement of leachates from dumpsites into the aquifer, and water milling (Akinseye et al., 2023; Odesa et al., 2024). One cannot overstate the importance of creating a system for safeguarding and managing such a crucial resource. Most of Nigeria's household water supply comes from groundwater, mainly from its closer proximity to end users and its lower development costs (Eyankware et al., 2023). Groundwater resources must be developed and safeguarded against contamination in order to fulfill the increasing demand for water and guarantee sustainable access to sufficient and clean water. The permeability, porosity, and overburden thickness of geologic formations play a major role in the groundwater's vulnerability to contamination from external sources (Obiora et al. 2015). Over the past ten years, there has been a rise in the use of geophysical techniques, particularly VES, for the assessment of hydrogeological sites (Vereecken et al., 2004; Herckenrath et al., 2013; Mosuro et al., 2017). The method is commonly employed because of its portability, speed, and reduced ambiguity in data interpretation. It is also non-destructive and environmentally friendly (Todd and Mays 2005; Adeniji et al. 2014), and it has been used to address hydrogeological issues (Faneca Sanchez et al. 2013; Burschil et al. 2012). One powerful geophysical technology that is frequently used for groundwater research is the electrical resistivity approach. According to Eyankware et al. (2022a), it offers details on the lithology and underlying structures. Reliable data regarding the shallow subsurface layers can be obtained by using the vertical electrical sounding (VES) approach. Mosuro et al. (2016) determined that aquifers surrounding dumpsites have low protective capacity and are vulnerable to leachate pollution by evaluating groundwater vulnerability to leachate infiltration using the electrical resistivity approach. The aquifer protective capacity and soil corrosivity in Delta South, Delta State, were assessed by Umuyah and Eyankware (2022) using the electrical resistivity method. To preserve the hydrological conditions, they designated locations for the placement of companies and the laying of iron pipes. With the use of geo-electrical research, Adeniji et al. (2014) assessed the aquifer protective capacity and soil corrosivity in the Bwari Basement Complex area of Abuja. They classified the area into four categories: good, moderate, weak, and poor. Nevertheless, researchers studying aquifer protective capacity, including Abiola et al. (2009), Atakpo and Ayolabi (2009), Ehirim and Nwankwo (2010), and Akana et al. (2016), could not find a relationship between an aquifer's rate of vulnerability and the quality of its groundwater for drinking. The ability of the overburden unit to delay and filter percolating ground surface-polluting fluid into the aquifer units is known as aquifer protective capacity (APC) (Adeniji et al. 2013). Therefore, it is necessary to assess the quality of the groundwater and determine whether areas with high APC correlate to areas with excellent or good water for drinking purposes, and vice versa. The aquifer protection units of the sandstone aquifers in the

Niger Delta Basin will be identified using electrical resistivity techniques, which will also be used to evaluate the hydrochemical properties of the groundwater. Finding places for service pipe burial that are noncorrosive, have acceptable water quality, and protect aquifers is the goal. In light of the expanding population and heightened groundwater exploration in Isoko, Patani, and its surroundings, as well as the necessity of sustainable groundwater management and ensuring access to sufficient and safe water, this is being done.

Location, climate, and topography of the study area

The research region is situated in the South-South geopolitical zone's Delta-Uzere State's community, a part of the Isoko metropolis. The Niger Delta region is a significant source of oil and gas. With headquarters in Oleh and Ozoro, respectively, the Isoko metropolis is divided into the Isoko-South and Isoko-North major local governments. Due to a high rate of oil spills, the Isoko-South Local Government Area (case study) in the Niger Delta has a high potential for oil wells. It is located in Delta State between longitudes 06^0 10'E and 06^0 18' E and latitudes $05^0$20'N and 05026'N (Fig. 1). Isoko-South L.G.A. is an Isoko indigene who lives in the southern part of Delta State. It has a total population of 235,147 people and covers an area of approximately 668 km2 (258 sq mi). 115,980 females and 119,167 males are present, according to the Delta State population census from 2006. It is nevertheless conveniently reachable via the river and road networks. Even though the terrain is rugged, it appears motorable during the dry season, and during the wet season, getting to the well heads and some of the nearby places can be a problem.

Geological setting of the area

The research area and its environs are part of the Niger Delta basin's Cretaceous to Recent clastic sediment piles, which are made up of the Agbada Formation, the Akata Formation, the Benin Formation (oldest to recent), and occasionally the Somebreiro Warri Deltaic Plain Sands (Allen, 1965; Reyment, 1965; Short and Stauble, 1967). The base of the Niger Delta stratigraphic sequence, the basement complex, is where the Akata Formation sits unevenly. Paleocene in age, the deposit is roughly 7000 m thick. The oil reservoir of the Niger Delta basin is the Eocene Agbada Formation, which is roughly 3700 meters thick and consists of an alternating succession of deltaic sands and shales. The Oligocene Benin Formation is made up of very porous gravels and sands with a few clay intercalations. According to Etu-Efeotor and Akpokodje (1990), the highest section is quaternary in age, 40–150 m thick, and consists of alternating phases of sand and silt/clay, with the latter becoming more noticeable as one approaches the coast. The most abundant aquifer in the Niger Delta is located in the Benin Formation, which varies in thickness and is over 2000 meters deep. It is particularly shallow in the northern section of the study area. The study region is situated beneath the Quaternary Somebreiro-Warri Deltaic Plain Sand. (Wigwe, 1975).

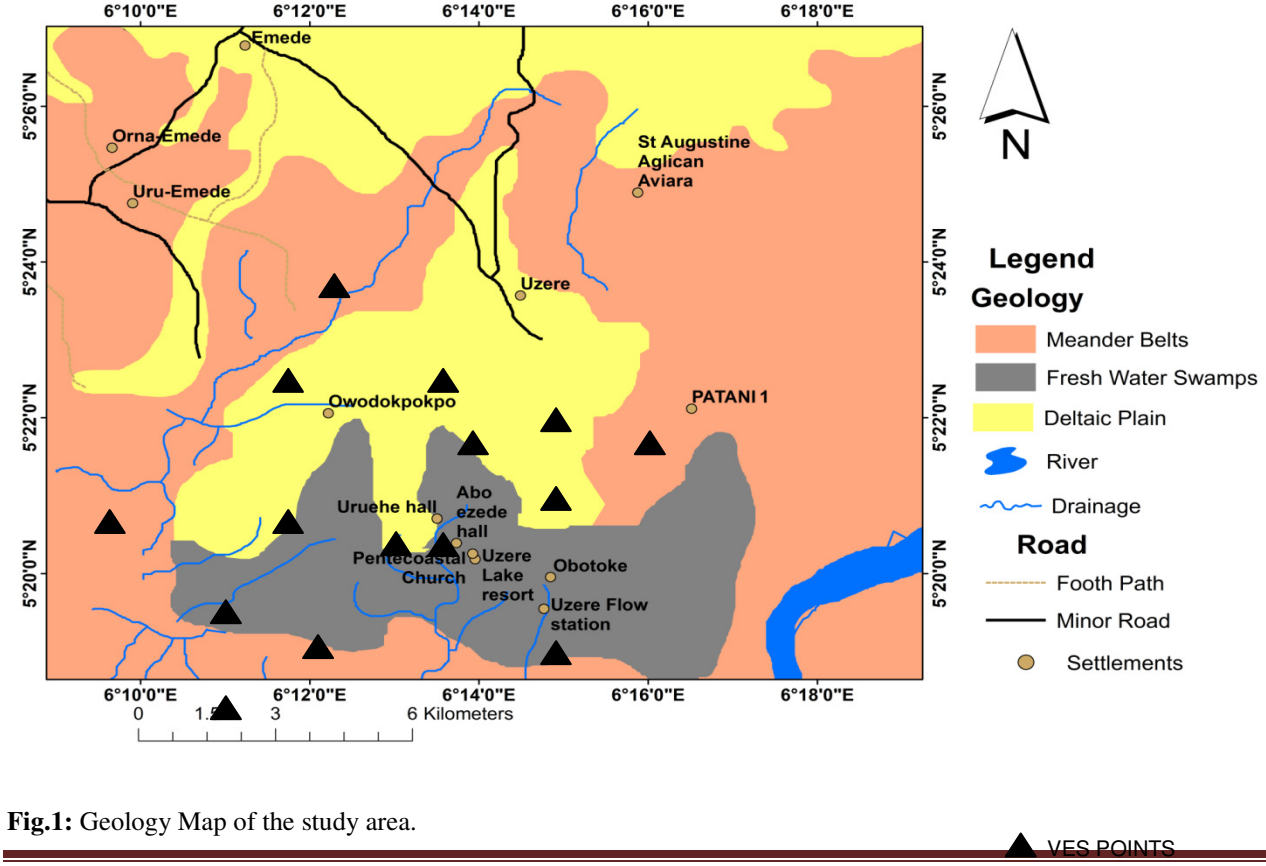

Fig.1: Geology Map of the study area.

Materials and methods

Investigation was conducted into the subsurface using ABEM SAS 1000 Terrameter. VES technique employing the Schlumberger electrode configuration was used for data acquisition. This involves the injection of measured low- frequency direct current (DC) into the subsurface via a pair of current electrode (AB) and measuring the corresponding voltage drop via another pair of potential electrode (MN). The depth of penetration is proportional to the separation between the current electrodes in homogeneous subsurface, while varying the electrodes separation provides information about the stratification of the ground (Batte, et al., 2010; Obiora et al. 2015). Current electrode spacing (AB/2) varied from 1 m to 400 m, while potential electrode separation was varied between 0.5 m and 25 m. The apparent resistivity was computed using (Ibuot et al. 2013):

Geoelectric measurements

With the aid of an Abem Terrameter SAS 1000 and its accessories, sixteen (16) VES were carried out inside the study region, as depicted in Fig. 1. A Schlumberger electrode array was utilized for each VES profile, with a maximum electrode separation of 100 m for half current (AB/2) and 5 m for half potential (MN/2). The spatial distribution of S, Tr, L, and pt was mapped using the Surfer program. The field data was observed, and apparent resistivity (a) values were calculated using equation (1) as follows:

$$\pi\left(\begin{matrix}\left(\frac{AB}{2}\right)-\left(\frac{MN}{2}\right)\\ MN\end{matrix}\right)\Delta V/I \qquad (1)$$

The apparent resistivity values were plotted against the current electrode spacing (AB/2) to create the geoelectrical curves. The development of sound curves was made possible by the use of the IX1D program, which aided in the data processing. The geoelectrical sections, which were created using the data from the sounding curves, were used to determine the aquifer's thickness. Using the charts provided by Loke (1999), lithologies that matched the geoelectric section were determined. Some elements related to the various combinations of the thickness and resistivity of the geoelectric layer are essential for the study and understanding of the geologic model (Zohdy et al. 1974; Maillet, 1947).

Dar Zarrouk's longitudinal (S) and transverse (T) parameters are derived via

$$S = \frac{h}{p} \qquad (2)$$

$$T = hp \qquad (3)$$

Using the formula below, we determined the total Longitudinal Unit Conductance (S).

The total longitudinal conductance is equal to the number of layers (n).

$$S = \sum_{i=1}^{n}\frac{h_i}{\rho_i} = \frac{h_i}{\rho_i} + \frac{h_2}{\rho_2} + \cdots + \frac{h_n}{\rho_n} \qquad (4)$$

as proposed by Asfahani (2012); Oli et al. (2020)

For the equation below, the Transverse Unit Resistance (Tr) was determined.

The total resistance of the transverse unit is

$$Tr = \sum_{i=1}^{n} h_i\rho_i = h_i\rho_i + h_2\rho_2 + \cdots + h_n\rho_n \qquad (5)$$

as proposed by Oli et al. (2020); Nwachukwu et al. (2019)

Below is the average longitudinal resistance for a given VES points

$$\rho_L = \frac{H}{S} = \frac{\sum_{i=1}^{n} h_i}{\sum_{i=1}^{n}\frac{h_i}{\rho_i}} \qquad (6)$$

as proposed by Suneetha and Gupta (2018).

The equation is used to calculate the Transverse Resistance for a particular VES curve.

$$\rho_t = \frac{T}{H} = \frac{\sum_{i=1}^{n} h_i \rho_i}{\sum_{i=1}^{n} h_I} \quad (7)$$

as proposed by Suneetha and Gupta (2018).

Equation 8 can be used to define the coefficient of anisotropy, a useful characteristic of an anisotropic media that shows the degree of fracturing.

$$\lambda = \sqrt{\frac{\rho_t}{\rho_L}} = \frac{\sqrt{ST}}{H} \quad (8)$$

When interpreting sounding data, the parameters T and S—transverse resistance and longitudinal conductance, respectively—are crucial. The Dar-zarrouk parameters are those that are displayed in Equations 1 through 5.

$$K = 0.0538E^{0.0072p} \quad (9)$$

Where is the aquifer layer resistivity

Transmissivity (T) is the product of the hydraulic conductivity (k) and the aquifer layer thickness.

$$T = K \times h \quad (10)$$

Each apparent resistivity value computed from the above equation was plotted on a log–log graph to the corresponding current electrode spacing, from which the layer resistivies, depths, thicknesses and curve types were deduced. The conventional quantitative interpretation using partial curve matching was done by matching the field curves with the auxiliary curves. Computer modelling software IX1Dwas used in the inversion and iteration of each VES point from which the resistivities and thicknesses of the layers were improved.

Result and Discussion

Figs 2, and 3 are interpretation of VES points 4 and 12 using IX1D software

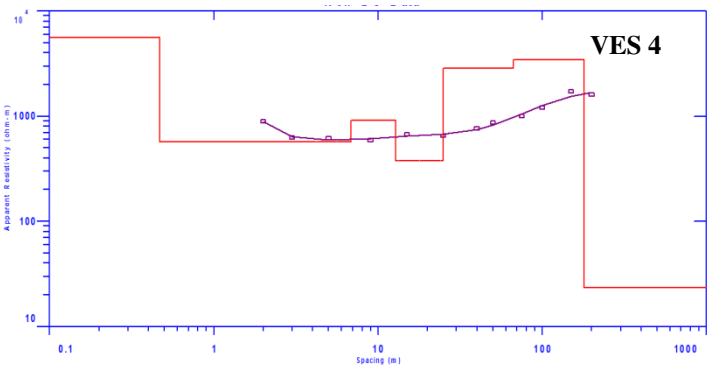

Fig. 2: Graph of VES 4.

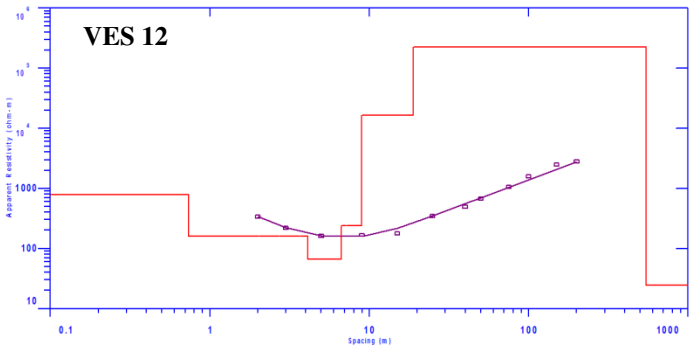

Fig. 3: Graph of VES 12

Table 1 Representative results of interpreted layer parameters from the study area

	Layers (m)	Resistivity (Ohm-m)	Thickness (m)	Depth (m)	Curve type
1	1	1305.6	3.0573	3.0573	QQ
	2	133.76	7.7981	10.855	
	3	843.85	11.579	22.434	
	4	8.5237	35.054	57.489	
	5	1545.2			
2	1	3884.6	2.2896	2.2896	H
	2	1040.2	2.1035	4.3931	
	3	7.1397	6.0824	10.476	
	4	89.418	105.95	116.43	
	5	26.750			
3	1	2147.3	2.1035	2.1035	HA
	2	475.13	2.5245	4.6280	
	3	3237.1	3.9399	8.5679	
	4	156.04	9.2438	17.812	
	5	7656.4	17.601	35.412	
	6	47632	311.48	346.90	
	7	26.207			
4	1	5552.7	0.46883	0.46883	QH
	2	569.85	6.3831	6.8520	
	3	911.57	5.9963	12.848	
	4	377.71	12.093	24.941	
	5	2835.2	41.853	66.804	
	6	3423.6	112.81	179.61	
	7	23.358			
5	1	3698.8	0.5177	0.5177	HA
	2	421.04	2.95110	3.4687	
	3	3353.3	6.7680	10.237	
	4	237.80	9.6856	19.922	
	5	2722.8	15.399	35.321	
	6	18351	239.77	275.09	
	7	24.846			
6	1	3663.6	0.464		HA
	2	659.84	3.7565		
	3	3966.8	6.3082		
	4	418.93	10.888		
	5	3243.9	31.031		
	6	53176	378.65		
	7	30.753			
7	1	340.10	1.9056	1.9056	AQ
	2	679.28	6.1806	8.0862	
	3	1453.2	6.3083	14.395	
	4	484.07	12.347	26.742	
	5	5311.2	31.654	58.396	
	6	237.70	59.443	117.84	
	7	17.020			
8	1	204.71	1.099	1.0999	AQ
	2	13342	0.27372	1.3736	
	3	164.24	0.45486	1.8285	
	4	6866.9	2.3346	4.1630	
	5	793.24	16.844	21.007	
	6	2279.1	52.737	73.744	
	7	520.19			
9	1	492.47	1.819	1.819	AH
	2	2734.7	1.448	3.267	
	3	507.29	3.444	6.712	
	4	4799.1	8.076	14.788	

	5	745.82	54.502	69.290	
	6	3338.0	198.29	267.58	
	7	25.928			
10	1	284.50	1.0631	1.0631	HA
	2	53.279	5.6988	6.7618	
	3	349.57	2.6888	9.4506	
	4	34012	3.9662	13.417	
	5	65.096			
11	1	778.22	0.73696	0.7369	**AH**
	2	160.72	2.5870	4.1119	
	3	66.171	2.2707	6.6989	
	4	237.55	9.9571	8.9696	
	5	16518	528.00	546.93	
	6	0.2268			
	7	24.577			
12	1	560.48	0.85568	0.85563	HA
	2	46.730	2.2622	3.1179	
	3	183.65	2.7400	5.8578	
	4	707.26	6.3237	12.181	
	5	1370.8	116.20	128.38	
	6	1135.6	263.72	392.10	
	7	21.262			
13	1	339.88	0.476	0.4763	QA
	2	25.092	4.2665	4.7428	
	3	7.2053	8.3626	13.105	
	4	71.608	5.9549	19.060	
	5	7.7478	45.805	64.865	
	6	1180.4	379.87	444.73	
	7	21.303			
14	1	125.63	5.7130	5.7130	A
	2	440.74	84.2941	90.004	
	3	3884.5			
15	1	107.91	0.79603	0.79603	
	2	150.46	2.0572	2.8532	AA
	3	89.914	3.0798	5.9331	
	4	1144.2	8.0594	13.993	
	5	228.90	39.226		
	6	6537.32	210.26		
	7	21.792			
16	1	50.915	1.3669	1.3669	HA
	2	113.14	1.3081	2.6750	
	3	10.988	2.6388	5.3138	
	4	258.39	11.841	17.155	
	5	53.164	49.679	66.831	
	6	2447.6	548.82	615.66	
	7	21.158			
17	1	147.20	2.422	2.422	HH
	2	68.112	3.042	5.4649	
	3	253.02	1.7508	7.2157	
	4	875.93	5.079	12.295	
	5	40.764	15.763	28.063	
	6	0.112	837.47	865.53	
	7	29.714			
18	1	81.072	1.3723	1.3723	HA
	2	57.221	4.3645	5.7368	
	3	219.75	2.141	7.8700	
	4	609.15	5.577	13.456	
	5	17.090	19.233	32.689	
	6	5210.4	553.27	585.96	

7 21.715

Table 2: Results of secondary parameters estimated from primary parameters

VES	Longitudinal Unit Conductance (*S*)	Transverse Unit Resistance (*Tr*)	Transverse Resistivity(ρt)	longitudinal resistance (ρL)	Hydraulic Conductivity (m/day)	Transmissivity (m^2/day)
1	4.186896	0	0	13.7307	3651.73687	0
2		0	0	5023.984	0.0538	0
3	0.069049	14836415	42768.57		4×10^{147}	1.4645E+150
4	0.064642	386216.3	2150.305	2778.519	2729647149	3.07931E+11
5	0.055553	4400019	15994.84	4951.852	1.29687E+56	3.1095E+58
6	0.042966	20135092	0	9535.021	1.0183E+165	3.856E+167
7	0.044549	168120.7	2878.977	1310.814	2.18012E+15	6.90096E+16
8	0.029733	120192.9	1629.867	2480.209	720022.8223	37971843.58
9	0.085772	661892	2473.623	3119.682	1473812162	2.92242E+11
10	0.11839	134898.4	10054.29	113.3289	1.2123E+105	4.8081E+105
11	0.093275	8721504	15946.29	5863.645	2.40575E+50	1.27024E+53
12	0.158566	299480.4	763.7859	2472.795	191.2991031	50449.39948
13	7.327213	448398.5	1008.249	60.69565	264.1185851	100330.7269
14	0.236731	0	0	380.1958	75388319652	0
15	0.233713	1374537	0	1067.487	1.48751E+19	3.12764E+21
16	1.258836	1343292	2181.873	489.071	2422324.534	1329420151
17	0.068035	4448.848	361.8421	180.7154	29.49480624	149.8041209
18	1.237495	2882758	4919.718	473.5051	1.05509E+15	5.83747E+17
Min	0.029733	0	0	13.7307	0.0538	0
Max	7.327213	20135092	42768.57	9535.021	1E+165	3.9E+167
Aver.	1.193072	3802618	7295.04	2624.421	1E+164	3.9E+166

VES survey

The summary of the interpreted VES survey is presented in Table 1. Findings from VES revealed geoelectric layers range from three to six layers with different intra-facies and inter-facies changes as shown in Table 1. The following curve types were deduced from modeling of VES data obtained from the field curve QQ, HA, AQ, AH, HH, QH, QA, A, and AA (Fig. 4). The variation in curve types showed the non-uniformity of resistivity trends across a study area and the non-uniformity of layering and alteration of layer properties as a result of geologic processes across study locations (Nwgoke 2013; Eyankware, et al., 2022b). The predominant curve type is the HK curve constituting about 37%; Q 28%; H 16%; HKA 11%; HHA and QQ each are represented by 8% see Fig. 4.

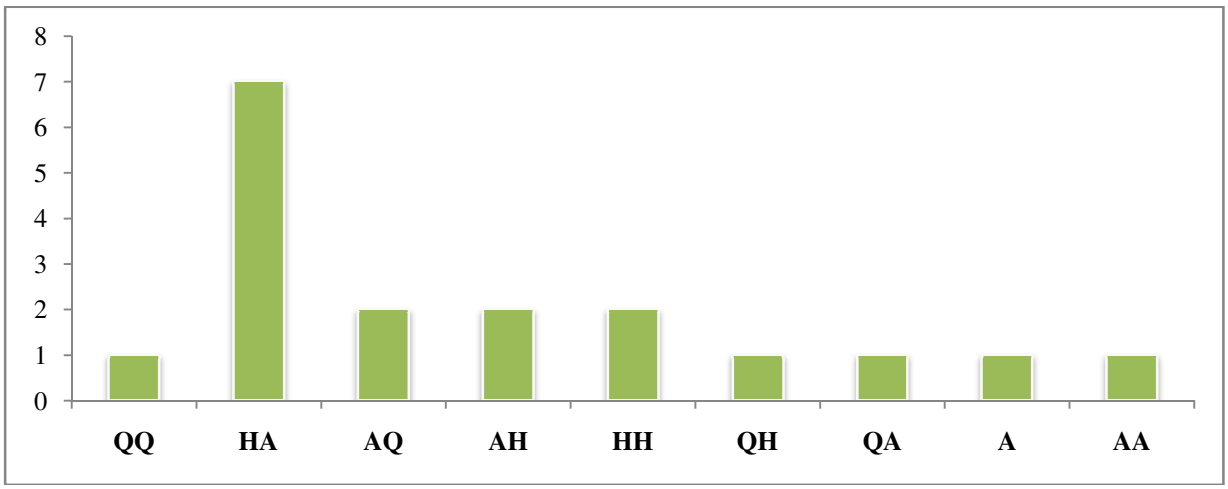

Fig. 4: Plot of VES points against Curve Type

Dar Zarrouk parameters of the study area

The aquifer protective capacity for the study area was computed as shown in Eqs. 2–7 and results of the estimated were presented in Table 2. Table 3 showed aquifer protective capacity rating. The longitudinal conductance (S) is one of the geoelectrical parameters used to determine target areas of the protective capacity of aquifer of the study area.

Longitudinal conductance (S)

Figure 5, b presents a spatial variation barchart of *S*. The map of *S* was prepared using the resistivity data of 20 sounding points. The estimated value of *S* varies from 0.029 Ω^{-1} at VES 8 to 7.327213 Ω^{-1} at VES13 see Fig. 5. Area around VES 8 with low S value indicate that the thickness of the overlain layer of the aquifer is considered not good enough to protect the aquifer from percolating fluid. The results of S obtained from the study was compared to the protective capacity rating model of Olusegun et al. (2016). From Table 3, it was observed that VES 3, 4, 5, 6, 7, 8, 9.10, 11, 12, and 17 fell within the poor category, that implies that water bearing unit within the aforementioned VES points are considered to be prone to surface contamination. Similarly findings conducted by Umayah and Eyankware, (2022) revealed that the vulnerability of aquifer to surface contamination in most Niger Delta areas can be attributed to the fact that the subsurface of the study area is underlie with permeability of the unconsolidated sands. Further deductions from Table 3, revealed that VES locations 12 was considered to prone to surface contamination. VES locations 14 and 15 fell within the moderate category, implying that the aquifer is moderately susceptible to surface contamination. While VES locations 1, 16, 18, and 13 fell within the good and excellent category this implies that aforementioned VES points are not non-susceptible to surface contamination.

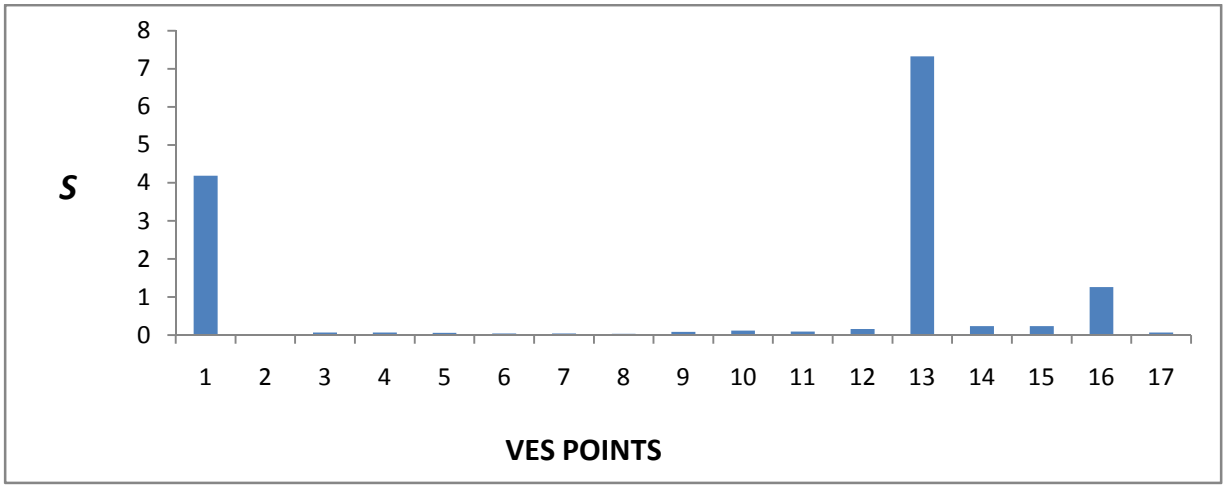

Fig. 5: Plot of VES against Longitudinal Conductance

Table. 3: Based on Oladapo and Akintorinwo's (2007) longitudinal conductance scale, modified aquifer protective capacity rating of the investigated formation (Henriet 1976)

Longitudinal conductance (mhos)	Protective capacity rating	VES Points
>10	Excellent	VES 13
5-10	Very Good	
0.7-4.9	Good	VES 1, 16, and 18
0.2-0.69	Moderate	VES/14 and 15
0.1-0.19	Weak	VES/ 1
< 0.1	Poor	VES/2,3,4,5.6,7,8,9,10, 11, 12, 13, VES/3, 4,5, 6, 7, 8, 9, 10, 11, and 17

Transverse Unit Resistance (*Tr*)

Tr is one of the geoelectric parameters used to defne the area of groundwater potential, (Nwachukwu et al. 2019). According to Okiongbo and Akpofure (2012) *Tr* of any subsurface geological formation is a product of resistivity and thickness. From transverse unit resistance values, it is also possible to determine the direction of flow of groundwater in the aquifer. It has a direct relation with transmissivity, the highest *Tr* values reflect the high transmissivity zone of the aquifers and vice versa

(Niwas and Singhal 1981, 1985). From Table 1, Tr has the least of 0 at VES 1, 2, 14, and the highest value of 20135092 at VES 6 see Fig.6. This implies that area of high Tr value has high prospect for groundwater.

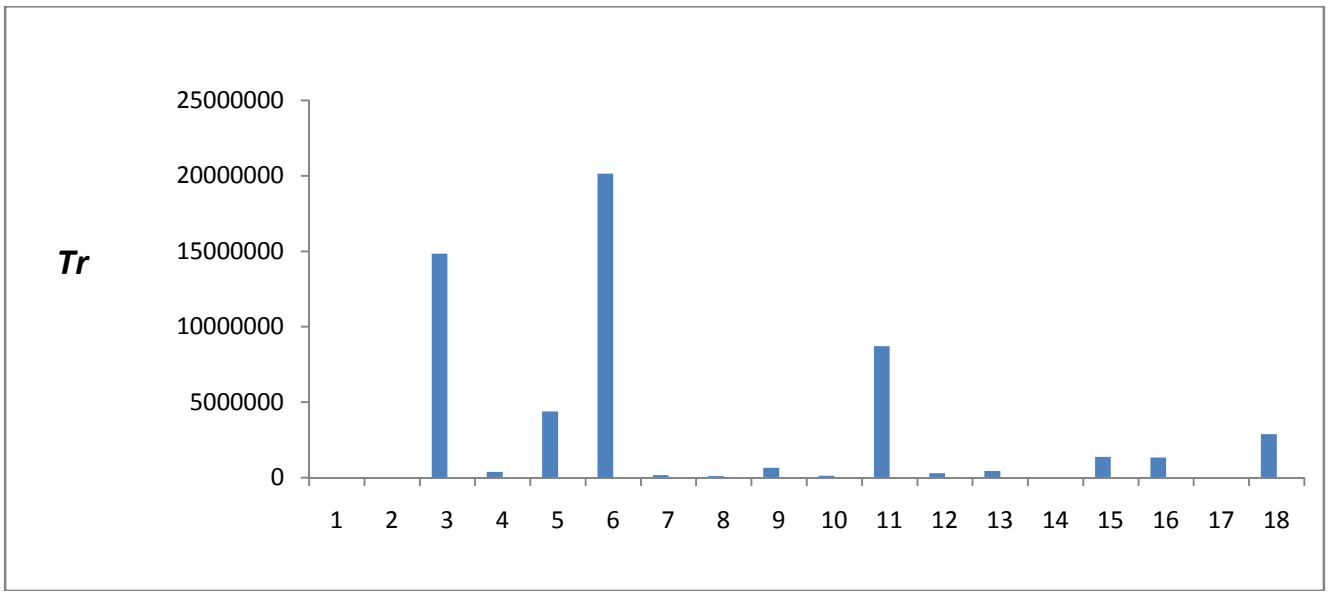

Fig. 6: Plot of VES against transverse unit resistance

Longitudinal Resistance (ρL)

The value of longitudinal resistance ranges from 13.7307 to 9535.02 Ω^{-m} with an average value of 2624.42 Ω-m as shown in Table 2. Fig. 7. This variation in longitudinal resistance , also demarcates different aquifers type into based on resistivity regimes (Gupta, et al. 2015).

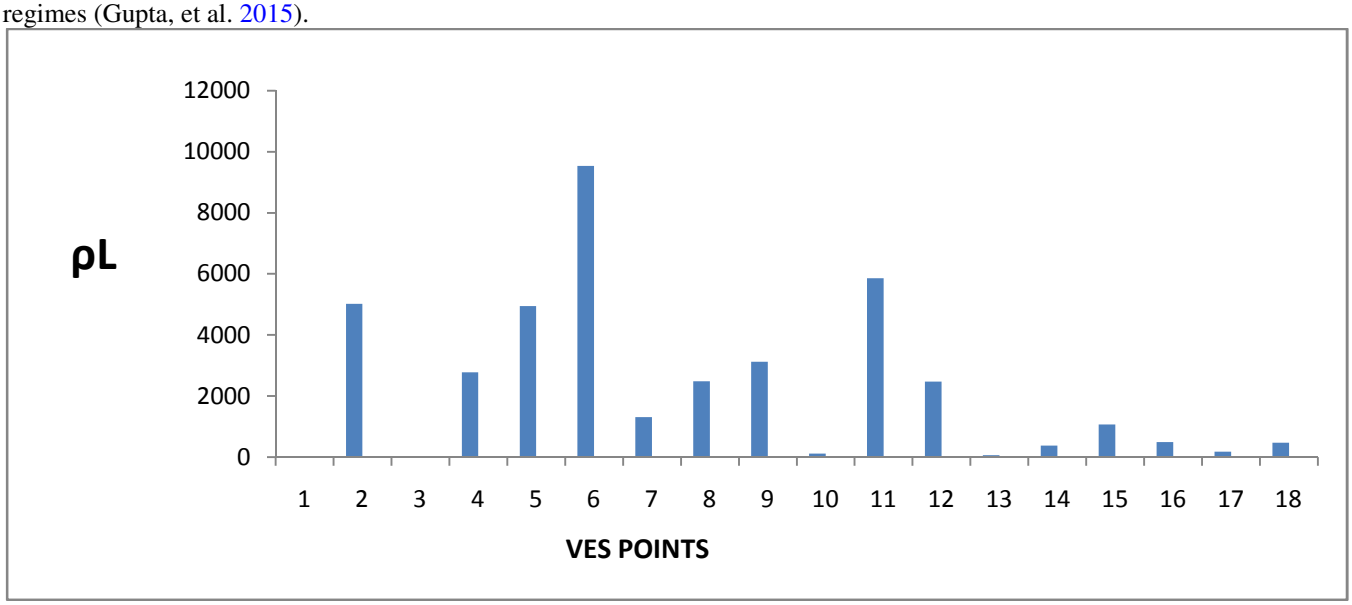

Fig.7: Plot of VES against longitudinal resistivity

Hydraulic conductivity (Kc)

The hydraulic conductivity of pore fluid determines how easy it can escape the compressed pore space. The capacity of the fluid to travel through the pores and cracked rocks is known as hydraulic conductivity of the material. Similarly, the conductivity of the water in a particular area is determined by the type of rock present. Obiora, et al. (2016) were of the believe that K controls the behaviour of groundwater flow within an aquifer. From Fig. 8, highest value of hydraulic conductivity was noticed at VES 7 as shown in Fig.8

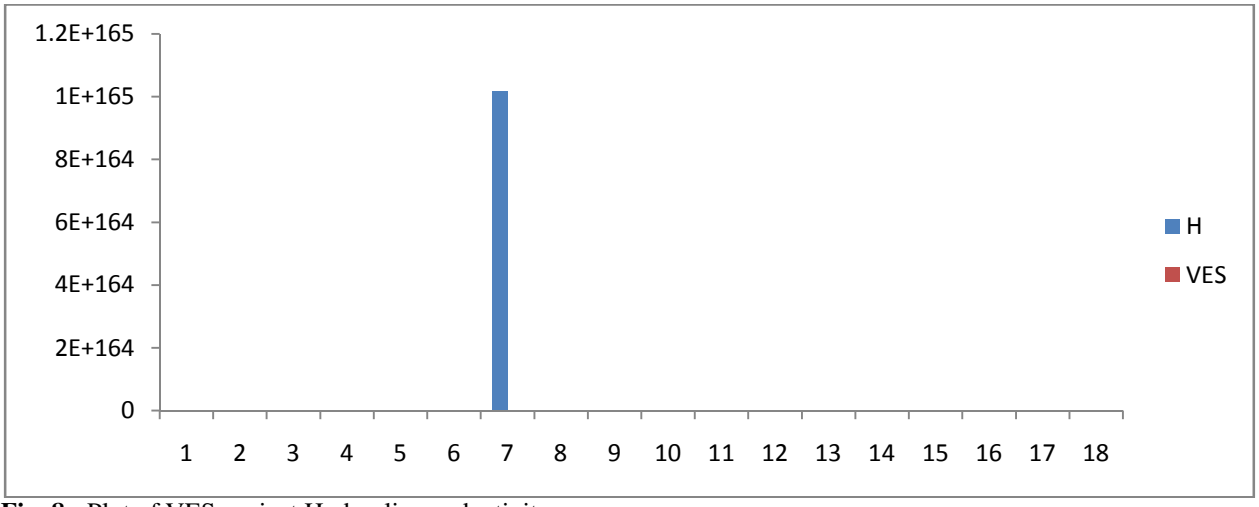

Fig. 8: Plot of VES against Hydraulic conductivity

Transmissivity (T)

T value for this study ranges from 0 to 3.97× $10^{167}\Omega/m^2$ with an average value of 3.910^{166} Ω/m^2; see Table 2. It has been observed that the transmissivity of water bearing unit is directly proportional to its transverse unit resistance. Hence, high Tr values correspond to high transmissivity values and vice versa (Henriet 1976; Ward 1990; Harb et al, 2010). The least value of T for this study was observed VES 1, 2, and 14 with value of 0, while the highest value was noticed at VES 6 with value of 3.97× $10^{167}\Omega/m^2$ see Fig. 9.

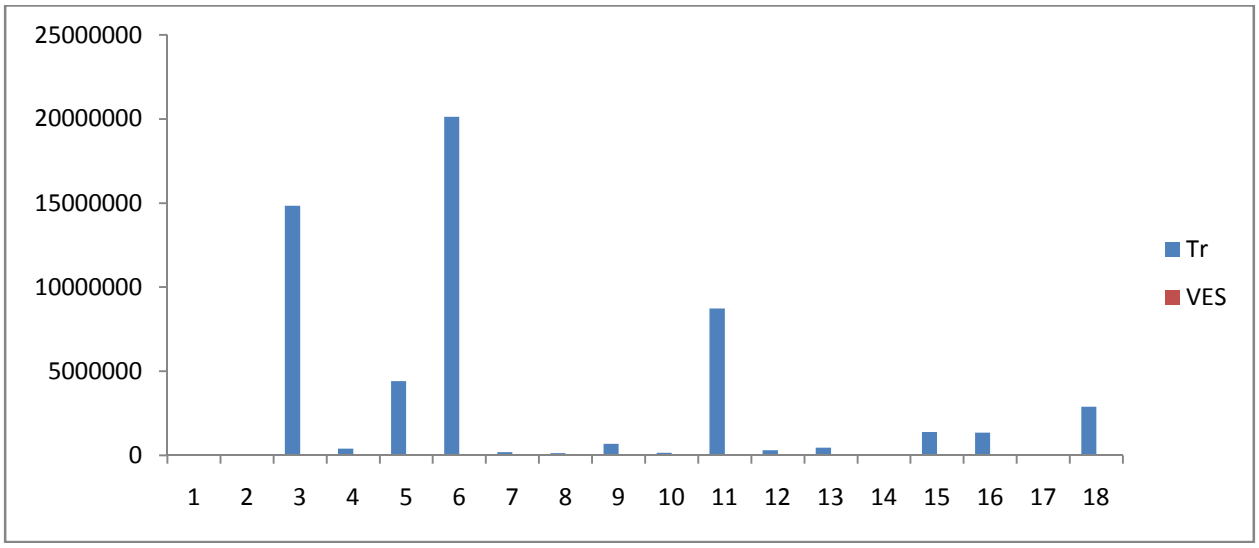

Fig.9: Plot of VES against Transmissivity.

Iso-resistivity interpretation across the study area

Iso-resistivity map using Golden Surfer 11.0 version was produced at specified AB/2 intervals, ranging from 6 m, 9 m, 40 m, 75 m, 75 m (repeated), 100 m and 150 m, as shown in Fig. 14a–g. It shows the colour range corresponding to resistivity values of the earth materials. Mbonu et al. (1991) stated that iso-resistivity maps are qualitative analysis tool that reveals possible variations in resistivity with depth at specific electrode spacing across a particular area, however, it does not give the true resistivity of a certain geo-electrical layer or unit. Since the effective depth of transmission is assumed to be about 2/3 of half of the current electrode separation (AB/2).

Iso-resistivity map (AB/2 at 3 m)

The AB/2 contour map of iso-resistivity strength at 6 m showed depth close to topsoil (Fig. 10). below shows that relatively high resistive materials underlay northwest parts of the study area within the resistivity value range of 100

to approximately 2700 Ωm in red, was seen in a limited section of the study area. Extremely low resistivity underlay southeast part of the study area with resistivity value of 0 to approximately 600 Ωm in violet in colour. High resistivity values are in red and white colour, with resistivity range of 2000 to 2700 Ωm as shown in Fig. 10.

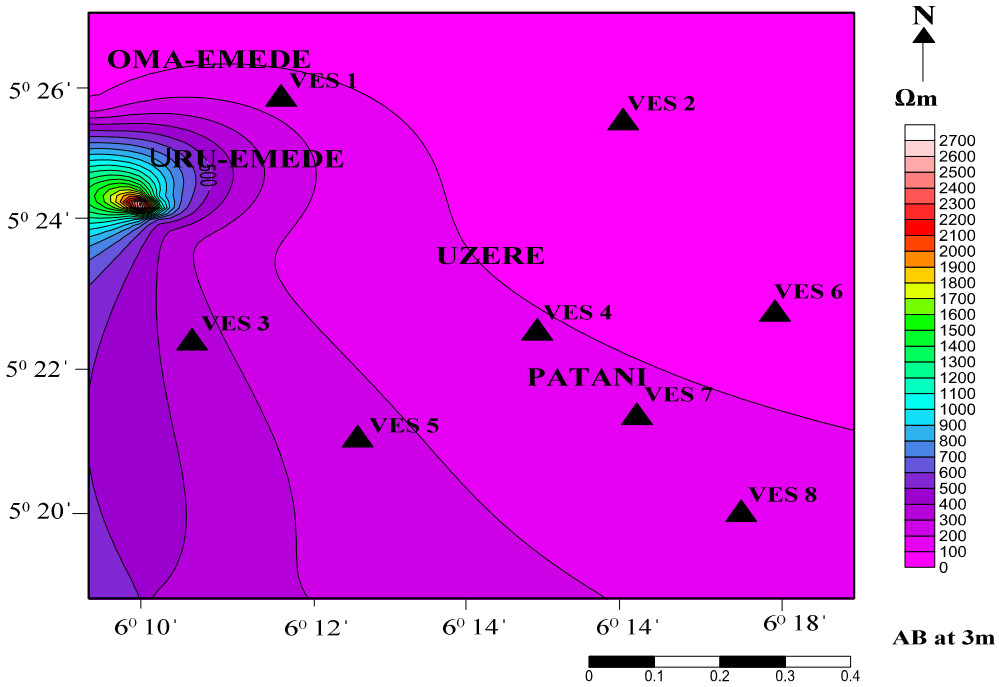

Fig. 10: Contour map of the iso-resistivity values across study area: **a** AB/2 = 3 m

Iso-resistivity map (AB/2 at 5m)

The AB/2 contour map of iso-resistivity strength at 5 m in Fig. 11 showed that most parts of the study area in the northern, eastern, western, and southeastern axes are underlined by relatively average/low resistive materials.

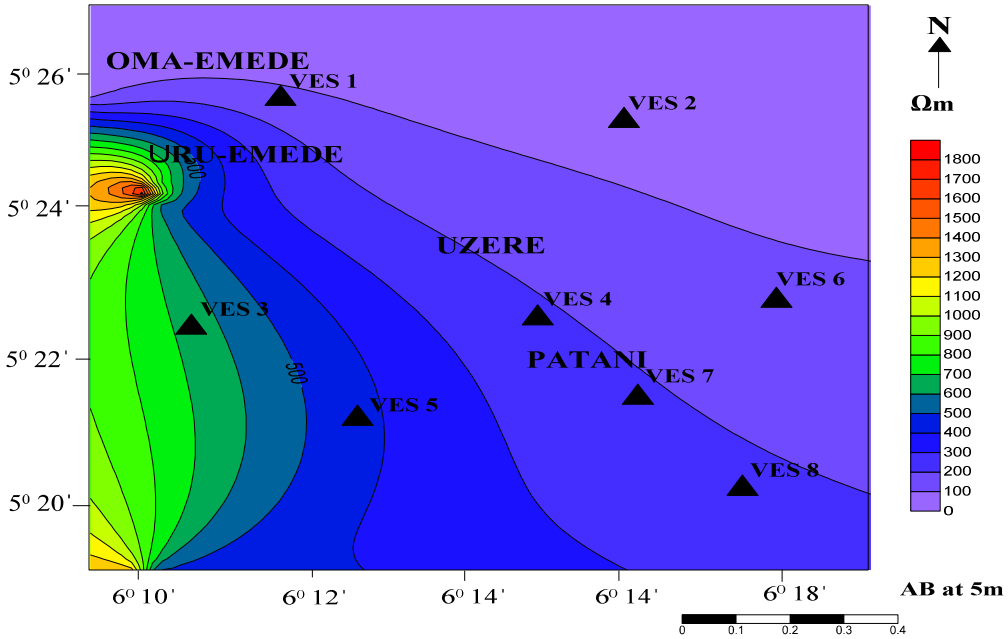

Fig. 11: Contour map of the iso-resistivity values across study area: **a** AB/2 = 5 m

Iso-resistivity map (AB/2 at 9m)

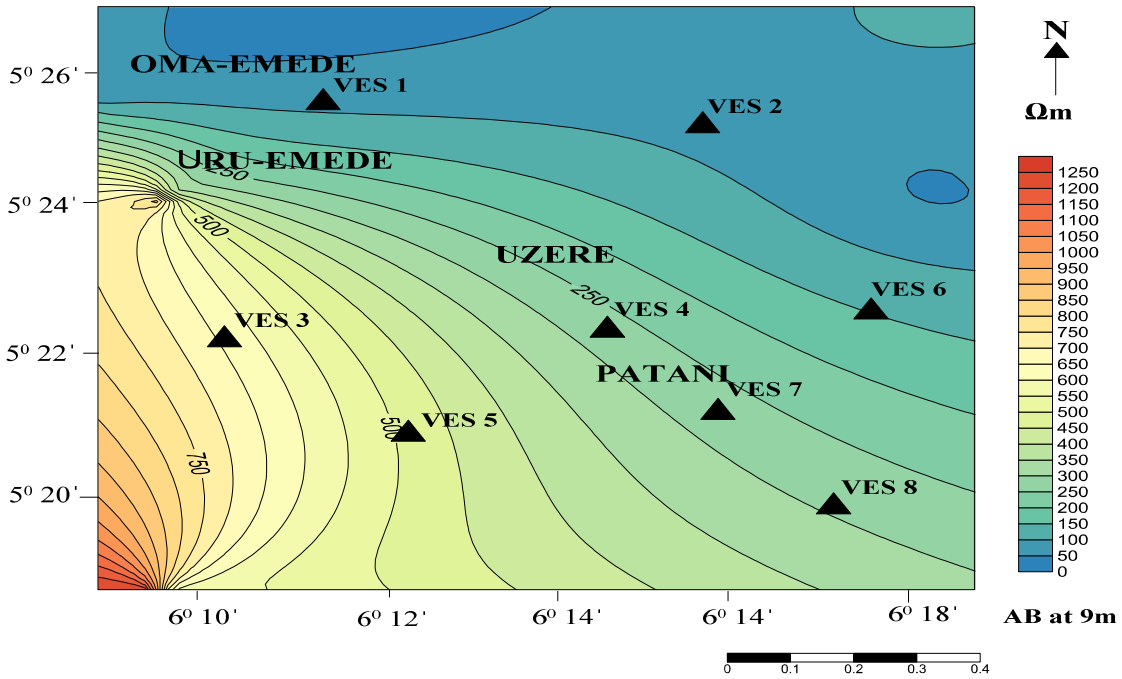

Fig. 12: Contour map of the iso-resistivity values across study area: **a** AB/2 = 9 m

Iso-resistivity map (AB/2 at 9m repeated)

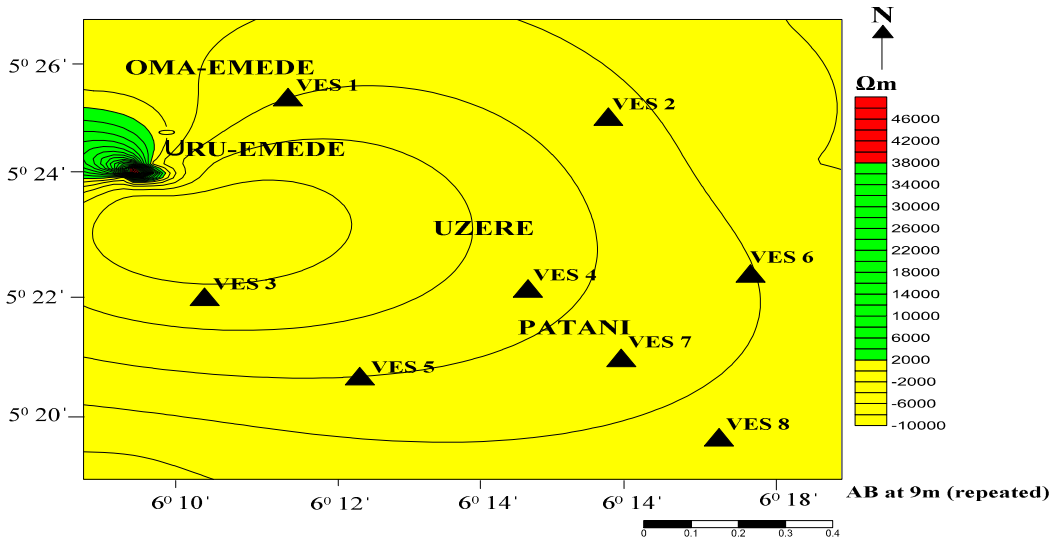

Fig. 13: Contour map of the iso-resistivity values across study area: **a** AB/2 = 9 m repeated.

Iso-resistivity map (AB/2 at 15m)

Fig. 14 Contour map of the iso-resistivity values across study area: **a** AB/2 = 15 m.

Iso-resistivity map (AB/2 at 25m)

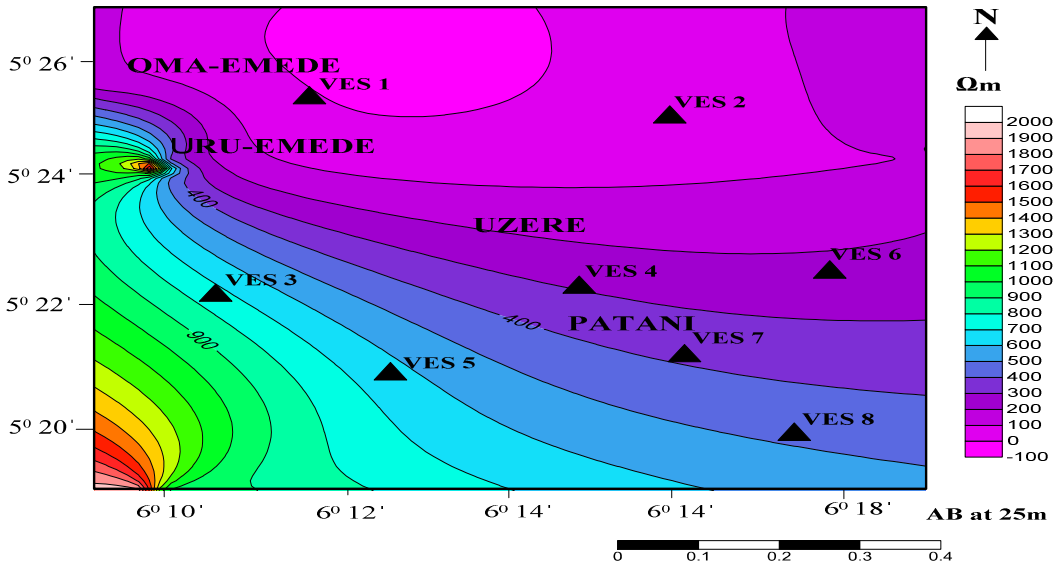

Fig. 15: Contour map of the iso-resistivity values across study area: **a** AB/2 = 25 m.

Iso-resistivity map (AB/2 at 40m)

The AB/2 contour map of iso-resistivity strength at 40 m in Fig. 16 showed that most parts of the study area in the southwest part of the study area is high in resistivity value with value range fo 1200 to 1700 Ωm, that is red and purple in colour. Areas of low resistivity value was observed around the northwest and northeast parts of the study area in blue color see Fig. 16. Findings from Fig. 15 showed AB at 25m showed that there is slight reduction in resistivity value of AB at 40 m when compared to AB at 25m.

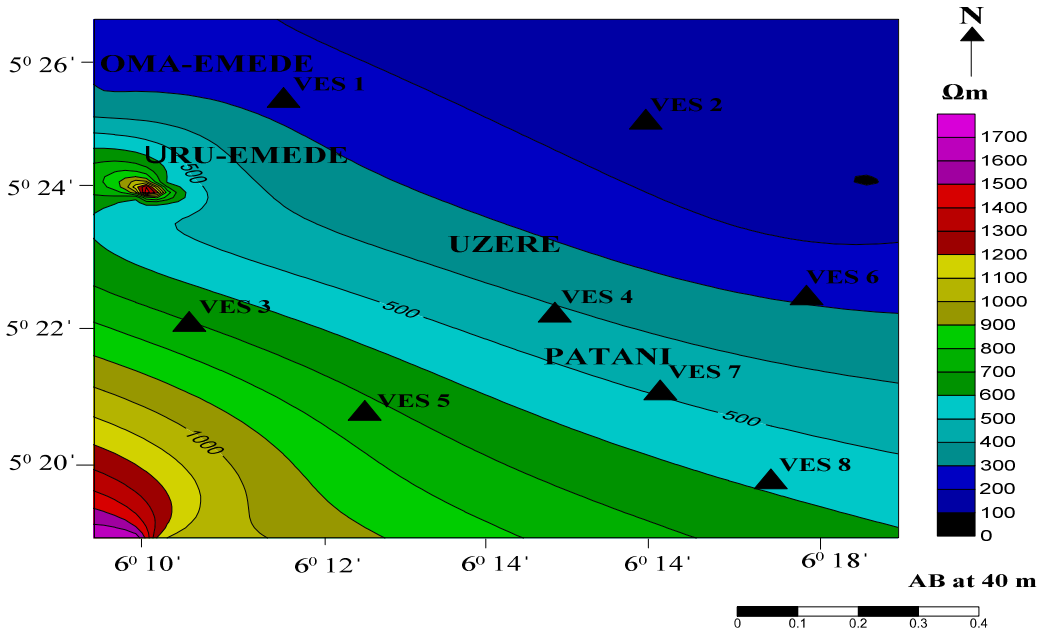

Fig. 16: Contour map of the iso-resistivity values across study area: **a** AB/2 = 40 m.

Iso-resistivity map (AB/2 at 50m)

The AB/2 contour map of iso-resistivity strength at 50 m in Fig. 17, below shows relatively high resistive materials underlay southwest axis of the study area with resistivity value ranging from 1200 approximately 1700 Ωm in red. While low resistivity value was observed around northwest parts of the study area with blue colour see Fig. 17.

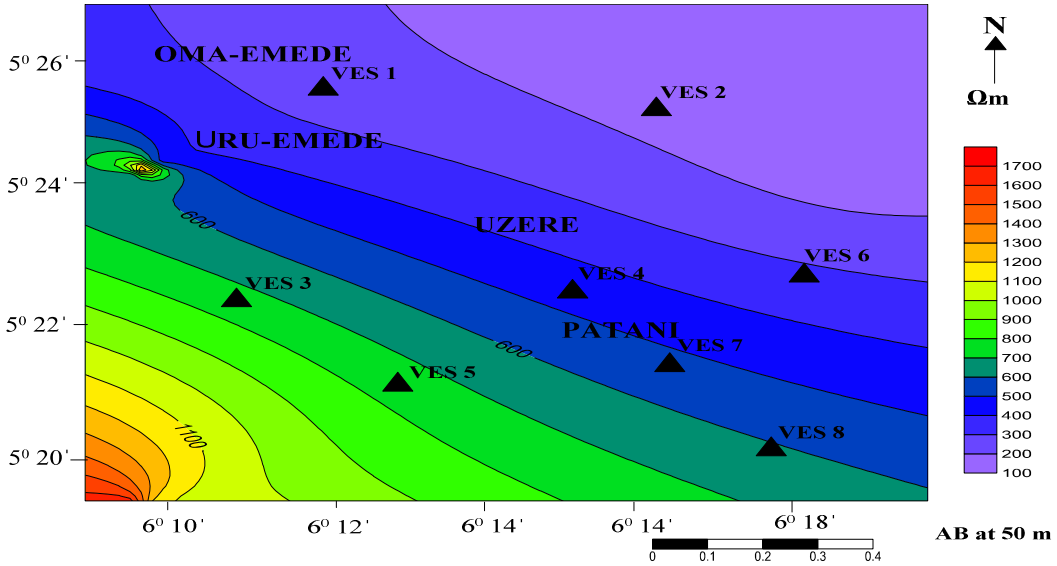

Fig. 17: Contour map of the iso-resistivity values across study area: **a** AB/2 = 50 m

Iso-resistivity map (AB/2 at 75m)

The AB/2 contour map of iso-resistivity strength at 75 m in Fig. 18, showed a trend of resistivity value that slightly increase when compared to AB/2 = 50 m. Fig. 18, below showed relative high resistive materials underlay the southwest of the study area with resistivity value range of 1500 to approximately 2000 Ωm in red, and white colour the northeast, part of the northeast and selected part of northwest in black with resistivity value of 0 to approximately 0 to 200 Ωm.

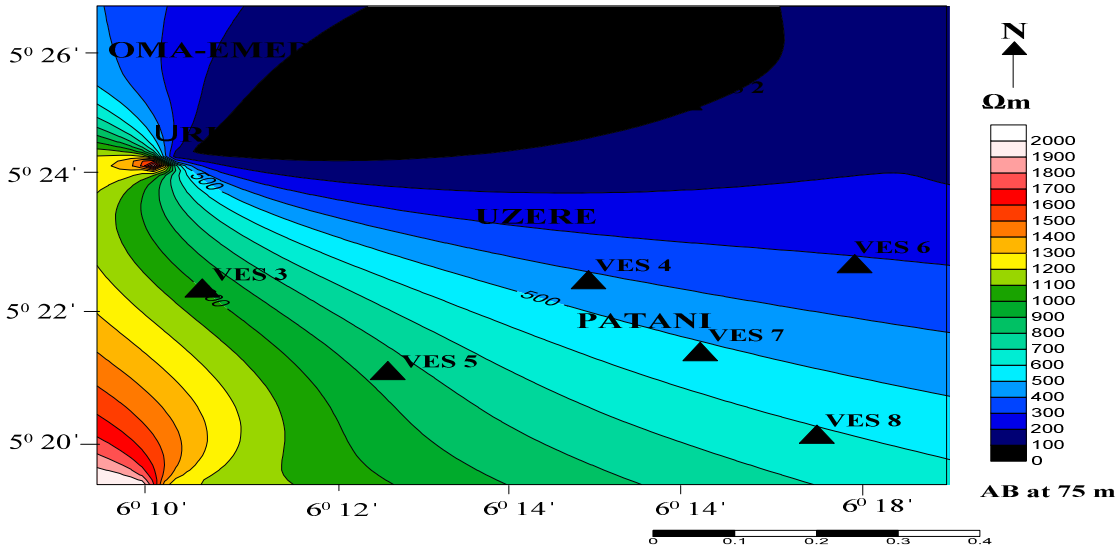

Fig. 18: Contour map of the iso-resistivity values across study area: **a** AB/2 = 75 m

Conclusion

Eighteen (18) VES were performed to identify the subsurface layer parameters (resistivity, depths, and thicknesses) that were used in determining Akure groundwater potential and aquifer vulnerability. Schlumberger electrode configuration was used for the survey, with a maximum half potential electrode separation of 10 m and a maximum half current electrode spacing of 100 m. Four curve types were identified in this study: QQ, HA, AQ, AH, HH, QH, QA, A, and AA. The interpreted geoelectric data revealed variations in the aquifer and Dar Zarrouk characteristics. The area's groundwater potential is generally modest, while the northern and western parts of the study area tend to have higher groundwater potential when compared to other parts in the study area as revealed by most of the maps generated. To enhance the existing groundwater resources in the study area, artificial recharging strategies, such as trenches, check dams, and percolation, are recommended.

References

Abiola, O., Enikanselu, P.A. and Oladapo, M.I. (2009).Groundwater Potential and Aquifer Protective Capacity of Overburden Units in Ado-Ekiti, Southwestern Nigeria. International Journal of Physical Sciences, 4, 120-132.

Adeniji, A. E., Obiora, D. N., Omonona, O. V., Ayuba, R. Geoelectrical evaluation of groundwater potentials of Bwari basement area, Central Nigeria. *International Journal of Physical Sciences*, 2013. 8(25), pp. 1350-1361

Asfahani J (2012) Quaternary aquifer transmissivity derived from vertical electrical sounding measurements in the Semi-Arid Khanasser Valley region. Syria. Acta Geophysica 60(4):1143–1158

Akakuru, C. A., Chidi, B. A., Diugo, O. I., Moses, O. Eyankware., Alexander, I. O., Adora, O. N., Kenneth, O. I., Ayatu, U. (2023). Application of artificial neural network and multi-linear regression techniques in groundwater quality and health risk assessment around Egbema, Southeastern Nigeria. Environmental Earth Sciences (2023) 82:77, https://doi.org/10.1007/s12665-023-10753-1,

Akinseye, V.O., · Osisanya, W.O., M. O. Eyankware., Korode, I.A.., Ibitoye, A.T. (2023). Application of second-order geoelectric indices in determination of groundwater vulnerability in hard rock terrain in SW. Nigeria. Sustainable Water Resources Management. 9:169, https://doi.org/10.1007/s40899-023-00936-w

Atakpo, E. A., Ayolabi, E. A. (2009). Evaluation of aquifer vulnerability and the protective capacity in some oil producing communities of western Niger Delta. The Environmentalist 29 (3), 310-317

Batte AG, Barifaijo E, Kiberu JM, Kawule W, Muwanga A, Owor M, Kisekulo J (2010) Correlation of geoelectric data with aquifer parameters to delineate the groundwater potential of hard rock terrain in Central Uganda. Pure appl Geophys 167(12):1549–1559

Ehirim, C.N. and Nwankwo, C. N. (2010). Evaluation of aquifer characteristics and groundwater quality using geoelectric method in Choba, Port Harcourt. Archives of Appl. Sci. Res., 2(2):396-403.

Eyankware MO, Akakuru CO, Eyankware EO (2022a) Hydrogeophysical delineation of aquifer vulnerability in parts of Nkalagu areas of Abakaliki, SE. Nigeria.Sustainable Water Res Manag, https://doi.org/10.1007/s40899-022-00603-6

Eyankware MO, Akakuru CO, Eyankware EO (2022b)Interpretation of hydrochemical data using various geochemical models: a case study of Enyigba mining district of Abakaliki, Ebonyi state, SE. Nigeria. Sustainable Water Res Manag. https://doi.org/10.1007/s40899-022-00613-4

Eyankware, M. O. Akakuru, O. C. Igwe, E. O, Olajuwon, W. O. Ukor, K. P.. (2024). Pollution Indices, Potential Ecological Risks and Spatial distribution of Heavy Metals in soils around Delta State, Nigeria. Water, air, & soil Pollution. https://doi.org/10.1007/s11270-024-07209-y

Gupta G, Patil SN, Padmane ST, Erram VC, Mahajan SH (2015) Geoelectric investigation to delineate groundwater potential and recharge zones in Suki River basin, north Maharashtra. J Earth Syst Sci 124(7):1487–1501

Harb N, Haddad K, Farkh S (2010) Calculation of transverse resistance to correct aquifer resistivity of saturated zones: Implications for estimating its hydrogeological properties. Lebanese Sci J 11(1):105–115

Henriet JP (1976) Direct application of Dar Zarrouk parameters in groundwater survey. Geophys Prospect 24:344–353
Ibuot, J. C., Akpabio, G. T., George, N. J. (2013). A survey of repository of groundwater potential and distribution using geoelectrical resistivity method in Itu L.G.A., Akwa Ibom State, Southern Nigeria. Central European Journal Geoscience, 5(4), 538- 554

Loke MH (1999) Electrical imaging surveys for environmental and engineering studies (A practical guide to 2-D and 3-D surveys). Minden Heights, Penang-Malaysia, pp. 57

Maillet R (1947) The fundamental equations of electrical prospecting. Geophysics 12:529–556

Masuro G.O., Omosanya, K.O., Bayewu, O.O., Oloruntola, M.O., Laniyan, T.A., Atobi, O., Okubena, M., Popoola, E. and Adekoya, F.(2016). Assessment of groundwater vulnerability to leachate infiltration using electrical resistivity method; applied water science, vol. 7, 2195-2207.

Ngwoke MO (2013) Determination of aquifer parameters in Ishiagu Ebonyi State using Geoelectric Method. Unpublished M.Sc Thesis, University of Nigeria, Nsukka

Niwas S, Singhal DC (1985) Aquifer transmissivity of porous media from resistivity data. J Hydrol JHYDA7 82:143–53J

Niwas S, Singhal DC (1981) Estimation of aquifer transmissivity from Dar-Zarrouk parameters in porous media. J Hydrol 50:393–399

Nwachukwu SR, Bello R, Ayomide O, Balogun AO (2019) Evaluation of groundwater potentials of Orogun, South-South part of Nigeria using electrical resistivity method. Applied Water Sci 9:184. https://doi.org/10.1007/s13201-019-1072-z

Obiora DN, Ajala AE, Ibuot JC (2015) Investigation of groundwater flow potential in Makurdi, North Central Nigeria, using surficial electrical resistivity method. Afr J Environ Sci Technol, 9(9):723–733

Obiora DN, Ibuot JC, George NJ (2016) Evaluation of aquifer potential, geoelectric and hydraulic parameters in Ezza North, southeastern Nigeria, using geoelectric sounding. Int J Environ Sci Technol 13:435–444. https://doi.org/10.1007/s13762-015-0886-y

Odesa, G. E., Elozona, O. E., M. O. Eyankware. (2024). A Review Study on Ecological Equity and Modern Remediation Techniques in Management of Soil. Journal of Pure and Applied Sciences.24.

Okiongbo KS, Akpofure E (2012) Determination of aquifer properties and groundwater vulnerability mapping using geoelectric method in Yenagoa City and Its Environs in Bayelsa State, South South Nigeria. J Water Resour Prot 4:354–362. https://doi.org/10.4236/jwarp.2012.46040

Oladapo MI, Akintorinwa OJ (2007) Hydrogeophysical study of Ogbese, southwestern. Niger Glob J Pure Appl Sci 13(1):55–56

OIi IC, Ahairakwem CA, Opara AI, Ekwe AC, Osi-Okeke I, Urom OO, Udeh HM, Ezennubia VC (2020) Hydrogeophysical assessment and protective capacity of groundwater resources in parts of Ezza and Ikwo areas, southeastern Nigeria. Int J Energy Water Resour. https://doi.org/10.1007/s42108-020-00084-3

Umayah OS, Eyankware MO (2022) Aquifer evaluation in southern parts of Nigeria from geo-electrical derived parameters. World News Nat Sci 42:28–43

Suneetha N, Gupta G (2018) Evaluation of groundwater potential and saline water intrusion using secondary geophysical parameters: A case study from western Maharashtra, India**.** E3S Web of Conferences 54:00033. https://doi.org/10.1051/e3sconf/20185400033

Ward, S.H. (1990) Resistivity and Induced Polarization Methods in Geotechnical and Environmental Geophysics. Society of Exploration Geophysicists, Tulsa, 147–189

Wigwe, G.A., 1975. The Niger Delta: physical. In: Ofomata, G.E.K. (Ed.), Nigeria in Maps: Eastern States. Pp380 - 400. Ethiope Publ. House, Benin City.

Zohdy AAR, Eaton GP, Mabey DR (1974) Application of surface geophysics to groundwater investigations. United State Geophysical Survey, Washington

